The Journal of Experimental Biology 210, 541-552
Published by The Company of Biologists 2007
doi:10.1242/jeb.02681

Trimethylamine oxide suppresses stress-induced alteration of organic anion transport in choroid plexus

Alice R. A. Villalobos[1,2,*] and J. Larry Renfro[1,3]

[1]*Center for Membrane Toxicological Studies, Mount Desert Island Biological Laboratory, Salisbury Cove, ME 04672, USA,* [2]*Environmental Medicine, University of Rochester, Rochester, NY 14642, USA and* [3]*Physiology and Neurobiology, University of Connecticut, Storrs, CT 06269, USA*

*Author for correspondence (e-mail: alice_villalobos@urmc.rochester.edu)

Accepted 5 December 2006

Summary

The effect of physicochemical stress on organic anion transport across the vertebrate blood–cerebrospinal fluid (CSF) barrier in the presence and absence of an endogenous cytoprotectant, trimethylamine oxide (TMAO), was investigated in isolated IVth choroid plexus (CP) of spiny dogfish shark (*Squalus acanthias*), an animal with naturally high levels of TMAO (~70 mmol l^{-1}). Active transepithelial absorption of the organic anion, 2,4-dichlorophenoxyacetic acid (2,4-D), by IVth CP mounted in Ussing chambers was measured after *in vitro* stress, and a marker for the cellular stress response, inducible heat shock protein 70 (Hsp70), was assayed by immunoblot analysis. Transient heat stress (a shift from the normal 13.5°C to 23.5°C for 1 h) decreased 2,4-D transport by ~66%; however, the same stress minus TMAO (isosmotic replacement with urea) had no effect on transport rate. In the absence of TMAO, stress-induced Hsp70 accumulation was more than double that seen in the presence of TMAO. Likewise, exposure to 50 μmol l^{-1} Zn for 6 h induced a twofold greater Hsp70 accumulation in the absence of TMAO than in its presence, and the higher Hsp70 level was associated with a higher 2,4-D transport rate. Heat stress and 50 μmol l^{-1} Zn also induced more pronounced increases in Hsp70 mRNA in the absence of TMAO. Thus, the cellular stress response can significantly alter CP organic anion transport capacity, and an endogenous osmolyte can suppress that response.

Key words: choroid plexus, heat shock response, Hsp70, 2,4-dichlorophenoxyacetic acid transport, dogfish shark, elasmobranch.

Introduction

The choroid plexus (CP) plays a key role in supporting neuronal function by secreting cerebrospinal fluid (CSF) and by modulating the levels of various soluble compounds such as organic anions (OAs). As the regulatory barrier at the interface of blood and CSF, the vertebrate CP is subject to physicochemical stresses and pathophysiological imbalances originating both peripherally and centrally. Factors that either impede or accelerate transport of potentially harmful compounds from the CSF by the CP are likely to impact health and neuronal function. Extreme stress is clearly damaging to the CP. For example, transient ischemia and subsequent reperfusion of rat CP markedly attenuate Na^+/K^+-ATPase activity and the capacity for glutamate accumulation (Ennis and Keep, 2006; Johanson et al., 2000; Palm et al., 1995). However, this brain barrier mounts a cellular stress response (Blake et al., 1990; Brown, 1991; Krueger-Naug et al., 2000), which in other tissues can be generally protective against physicochemical stressors such as ischemia, hyperthermia, oxidants or heavy metals and may ameliorate loss of function in CP.

An increased production of heat shock proteins (hsps) results from a variety of cellular stresses such as hyperthermia and exposure to heavy metals. Hsps are both chaperones that prevent premature folding of nascent proteins and cytoprotectants that preserve and restore native conformation of damaged proteins (Agashe and Hartl, 2000). Denatured or abnormal cellular proteins (misfolded) can signal an increased activation of the heat shock genes (Hightower, 1980; Ananthan et al., 1986; Hightower, 1991). The resultant increase in hsp accumulation can improve tolerance of subsequent stress of equal or greater severity, and such conditioning may predispose the cell or organism to survive an otherwise lethal stress. In many cases, the conditioning stress may preserve or enhance certain cell and tissue functions (Calabrese, 2005). This effect is associated with elevated cellular levels of hsps, especially Hsp70/72 (Brown et al., 1992; Renfro et al., 1993; Sussman-Turner and Renfro, 1995; Sussman and Renfro, 1997; Hightower et al., 2000), and

in several cases increased hsp levels have been shown to be necessary (Renfro et al., 1993; Riabowol et al., 1988) and sufficient (Heads et al., 1995) for this effect.

Like hsps, many organic osmolytes are also cytoprotectants and act to stabilize tertiary protein structure. Certain animal groups, such as marine elasmobranchs, maintain high systemic levels of osmolytes. Sharks naturally maintain plasma urea concentrations of 350–400 mmol l^{-1} and trimethylamine oxide (TMAO) concentrations of ~70–80 mmol l^{-1} (Goldstein et al., 1967). The intracellular ratio of urea:TMAO + glycine betaine is near 2:1, and these high levels of TMAO and glycine betaine counteract the protein destabilizing effects of urea in sharks (Somero, 1986; Yancey and Somero, 1979; Yancey and Somero, 1980). Examples of protein stabilizing effects of methylamines are also found in the mammalian renal medulla. Here, as in marine elasmobranchs, urea concentrations and ionic strength are high enough to destabilize macromolecules (400–600 mmol l^{-1}), yet the renal tubule cells survive and efficiently transport inorganic and organic solutes. Urea decreases the thermal transition temperatures of several critical proteins in the kidney, whereas the methylamines glycine betaine and glycerylphosphorylcholine increase them, effectively counteracting urea and, consequently, temperature-induced protein denaturation (Burg and Peters, 1998). TMAO also effectively restores the activity of certain enzymes lost by exposure to high urea (Palmer et al., 2000). Other relevant examples include the effective rescuing and restoration by TMAO of the dysfunctional cystic fibrosis transmembrane conductance regulator (CFTR) mutant F508 to functional capacity similar to that of the native protein (Brown et al., 1996). Proteins exhibiting temperature-sensitive folding defects, such as the tumor suppressor p53, viral oncogene protein pp60src and ubiquitin activating enzyme E1, are also restored to near-native phenotype by TMAO (Brown et al., 1997).

Through their protein stabilizing effects, the osmolytes can attenuate Hsp70 induction by hyperosmotic stress as well as temperature shock (Sheikh-Hamad et al., 1994). Thus, given that osmolytes may protect and salvage protein function in other transporting epithelia, we asked whether in CP high levels of osmolytes supplant the role of hsps and modify stress-induced changes. We had previously established the CP (IVth and lateral) of the dogfish as a model for direct assessment of transepithelial OA transport, demonstrating active removal or absorption of two model substrates [2,4-dichlorophenoxyacetic acid (2,4-D) and fluorescein] from the CSF compartment *via* a specific and Na^+-dependent pathway similar to the mechanism described for mammalian CP (Villalobos et al., 2002). The objective of the present study was to determine how physicochemical stress in the presence and absence of the endogenous cytoprotectant, TMAO, may alter OA transport across the vertebrate blood–CSF barrier. The data indicate that heat shock or zinc exposure can alter CP transepithelial OA transport and that TMAO diminishes both the induction of Hsp70 synthesis and the capacity to actively transport OAs under conditions of physicochemical stress.

Materials and methods

Animals

Adult male and female spiny dogfish sharks (*Squalus acanthias* L., ~2 kg body mass) were collected from the coastal waters of Mount Desert Island, Maine, USA and held in large (11 360 liters) tanks of flowing sea water 1–4 days before use. Experiments were conducted from the period June through July during which tank temperature ranged from 13 to 19°C. Animals were decapitated, and the cranial compartment immediately removed, flooded with ice-cold elasmobranch Ringer (ER; in mmol l^{-1}, 280 NaCl, 6 KCl, 4 $CaCl_2$, 3 $MgCl_2$, 1 NaH_2PO_4, 0.5 Na_2SO_4, 350 urea, 72 TMAO, 2.5 glucose and 8 $NaHCO_3$, pH 7.8) and placed on ice. With the cerebrum and medulla submerged in ice-cold sterile ER, the IVth and lateral plexuses were excised and cleared of extraneous tissue. Tissues were then either cultured for 48–72 h with or without TMAO for subsequent heat stress treatment or incubated without or with TMAO during treatment with zinc. The present study adheres to the newest Guiding Principles for Research as outlined by the American Physiological Society (American Physiological Society, 2002). All investigations involving animals reported in this study were conducted in conformity with these principles, and the animal protocol was approved by the Mount Desert Island Biological Laboratory IACUC (protocol #0606; MDIBL Institutional Assurance #A3562-01).

Explant tissue culture and heat stress treatment

The effects of TMAO on heat-induced modulation of transport and Hsp70 accumulation in IVth and lateral CP, respectively, were investigated *in vitro* using isolated tissues that were maintained in culture prior to initiation of heat stress. This provided a consistent thermal history prior to further treatment. Immediately following dissection, the IVth CP was bisected longitudinally, and each half-plexus was rinsed four times in sterile ER. Subsequently, one half-IVth CP was rinsed twice in sterile Leibovitz's (L-15) medium (Gibco, Invitrogen, Carlsbad, CA, USA) modified for use with elasmobranch tissues (L-15E) by supplementation with the following (in mmol l^{-1}): 142 $NaCl_2$, 2.75 $CaCl_2$, 2 $MgCl_2$, 350 urea and 72 TMAO. The contralateral half-IVth plexus was rinsed in TMAO-free L-15E medium in which TMAO was replaced isosmotically with urea. Each half-IVth plexus was placed in a 35 mm Petri dish with 3 ml of the respective L-15E medium at 13.5°C (humidified air) for a minimum of 48 h before initiation of stress treatments. Lateral plexuses were prepared in a similar manner. IVth and lateral CPs were heat-stressed in the same L15E medium in which they were cultured. Tissues were heated to 23.5°C for 1 h and then returned to 13.5°C for an additional 1.5 h. Corresponding non-heated tissues were similarly handled but held at 13.5°C continuously. At the end of treatment, IVth plexus tissues were mounted in Ussing chambers for measurement of [^{14}C]2,4-dichlorophenoxyacetic acid ([^{14}C]2,4-D) transport, and segments of lateral plexus were processed for immunoblot analysis of Hsp70 protein or semi-quantitative RT-PCR analysis of Hsp70 mRNA.

Zinc treatment

The influences of TMAO on zinc-induced alteration of organic anion transport and Hsp70 expression were examined in IVth and lateral CP *in vitro*. Following harvest, tissues were incubated for 6 h in either L15E or TMAO-free L-15E with or without 50 μmol l^{-1} $ZnSO_4$ (13.5°C, humidified air). L-15E medium does not contain zinc. Following exposure to zinc, all tissues (regardless of the presence of TMAO during zinc exposure) were rinsed twice with L-15E containing TMAO and allowed to recover in this complete medium for 1.5 h (13.5°C, humidified air). Tissues were then mounted in Ussing chambers for measurement of bioelectrical properties and transepithelial transport of [^{14}C]2,4-D. Lateral CPs were treated as described for IVth CP and processed for analysis of Hsp70 accumulation or Hsp70 mRNA.

Transepithelial transport

Ussing flux chambers were used to determine transepithelial transport and electrophysiological properties of IVth CP. In the dogfish, the IVth CP is a flat sheet of epithelial tissue overlying the dorsal and lateral surfaces of the medullary auricles. In a 2–3 kg animal, it is 3–4 cm^2 of choroidal epithelium that contains the tight junctional barriers. After treatment, each half-IVth plexus was transferred onto a piece of nylon mesh (Nitex®, 150 μm mesh size) and mounted in an Ussing chamber. Aperture size was 0.2 cm^2. Each hemichamber was filled with ER containing 10 μmol l^{-1} 2,4-D, continually gassed with humidified 99% O_2–1% CO_2, and magnetically stirred. Chamber temperature was maintained at 13.5°C.

Each flux chamber was attached to an automatic voltage clamp (Model EC4000-2; WPI, Sarasota, FL, USA) interfaced with a computer-controlled data acquisition board (MacLab, ADI Instruments, Grand Junction, CO, USA). Methods for determination of electrophysiological properties were described previously (Villalobos et al., 2002). Transepithelial electrical resistance (R_t) was used as an indicator of structural integrity. Transepithelial fluxes of 2,4-D were determined under short-circuited conditions, i.e. ER on both sides and transepithelial electrical potential clamped at 0 mV. Under control conditions, transepithelial potential difference, R_t and short-circuit current (I_{sc}) remained stable for at least four hours and were similar to those previously reported (Villalobos et al., 2002).

Unidirectional OA transport rates were determined by adding 3.7×10^4 Bq [^{14}C]2,4-D to the CSF-side or blood-side of each half-plexus as previously described (Villalobos et al., 2002). The net transepithelial flux of 2,4-D by a single IVth plexus was calculated by subtracting the blood-to-CSF (secretory) flux from the CSF-to-blood (absorptive) flux measured in its respective paired half (Fig. 1A). In some cases, non-mediated flux ('leak' flux) was determined after addition of 10 mmol l^{-1} *para*-aminohippuric acid (PAH) together with 100 μmol l^{-1} 2,4,5-trichlorophenoxyacetic acid (2,4,5-T). The remaining uninhibited flux was considered non-mediated, and previous work showed that it was equivalent to unidirectional blood-to-CSF flux (Villalobos et al., 2002) (Fig. 1B). Net

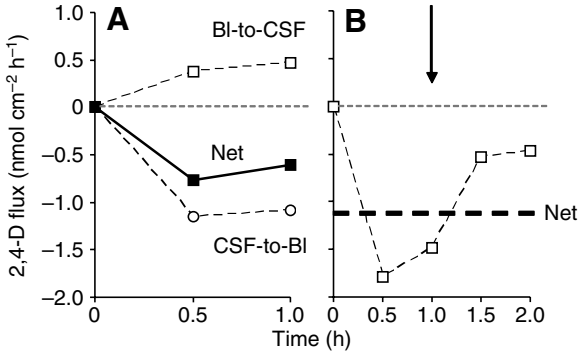

Fig. 1. Two examples of unidirectional and net fluxes of 10 μmol l^{-1} [^{14}C]2,4-dichlorophenoxyacetic acid (2,4-D) in freshly isolated shark IVth choroid plexus (CP) under short-circuited conditions. (A) Unidirectional absorptive [cerebrospinal fluid-to-blood (CSF-to-Bl)] and secretory [Bl-to-CSF] fluxes of 2,4-D in paired halves of IVth CP mounted in Ussing chambers under short-circuited conditions in elasmobranch Ringer solution. Fluxes were initiated at t=0 by addition of isotopically labeled 2,4-D. Steady-state flux was apparent by t=0.5 h. (B) Alternate method of determining unidirectional and net absorptive flux of 2,4-D in a single one-half IVth CP under short-circuited conditions. Flux was initiated at t=0 by addition of isotopically labeled 2,4-D to the CSF compartment without inhibitor. At t=1 h, 100 μmol l^{-1} 2,4,5-trichlorophenoxyacetic acid (2,4,5-T) was added to both blood and CSF compartments, and 10 mmol l^{-1} *para*-aminohippuric acid (PAH) was added only to the CSF compartment (arrow); unidirectional flux was measured for an additional hour. Net flux was calculated as the difference between the initial 1-h flux (total flux) and second 1-h flux (inhibitor-insensitive flux).

active fluxes of 2,4-D (CSF to blood) in control 48-h explants (0.3±0.11 nmol cm^{-2} h^{-1}) and freshly isolated CP tissue (0.4±0.05 nmol cm^{-2} h^{-1}) were nearly identical; however, transport rates by control 7.5-h explants averaged considerably higher than in either of the above (see controls in Figs 2, 4).

Immunoblot analysis

Hsp70 and actin in control and stressed lateral CP were compared by immunoblot analysis. After treatment, tissues were rinsed in chilled ER/0.5% Triton X-100 supplemented with phosphatase and protease inhibitors and then lysed with sample buffer (65 mmol l^{-1} Tris-HCl, pH 6.8, 5% v/v β-mercaptoethanol, 10% v/v glycerol, 2.3% w/v SDS, 0.5% bromophenol blue). Proteins in heat-denatured tissue lysates were separated by electrophoresis (SDS/10% polyacrylamide gel) then electroblotted onto polyvinylidene difluoride membranes. Membranes were then blocked with 10% milk protein in Tris-buffered saline containing 0.1% Tween-20 (TBS-T, 1.5 h, 24°C) followed by overnight incubation (4°C) in fresh blocking buffer with a mouse monoclonal primary antibody against either Hsp70/heat shock cognate 70 (Hsp70/Hsc70, 1:1000; Stressgen, Victoria, BC, Canada) or β-actin (1:500; Sigma-Aldrich, St Louis, MO, USA). For heat shock protein analysis, membranes were subsequently incubated in 5% milk/TBS-T with horseradish peroxidase-

conjugated secondary antibody against mouse IgG (1:1000; Santa Cruz Biotechnology, Santa Cruz, CA, USA; 24°C, 1.5 h); immunoreactivity was detected using a luminol-based chemiluminescent substrate (LumiGLO; Kirkegaard & Perry Labs, Inc., Gaithersburg, MD, USA) and visualized on X-ray film. For actin analysis, membranes were incubated with alkaline phosphatase-conjugated secondary antibody against mouse IgG (1:3000; Stressgen; 24°C, 1.5 h), and immunoreactivity was detected with chromogenic substrate, BCIP/NBT (Promega, Madison, WI, USA). For each tissue lysate sample, the relative area and intensity of individual Hsp70 and actin bands were quantitated by densitometry (NIH Image), and Hsp70 accumulation was normalized to that of actin.

The antibody used for analysis of Hsp70 protein is immunoreactive with both the inducible and constitutive forms of Hsp70 in mammals, i.e. two bands are detected in mammalian tissues. For shark tissues, only a single band was detected using this antibody; its mass most closely coincides with the constitutive or cognate form of mammalian Hsp70 (70 kDa).

Isolation of mRNA and RT-PCR

Relative levels of Hsp70 mRNA in non-treated and stressed tissue segments of lateral CP were analyzed by semi-quantitative RT-PCR. Total RNA was isolated from experimental tissues (RNeasy® Mini kit; Qiagen, Valencia, CA, USA). Briefly, tissue segments were triturated with guanidine isothiocyanate-containing buffer with 1% β-mercaptoethanol and homogenized using a QiaShredder® spin column (Qiagen). Ethanol was added to the homogenate, which was then loaded onto a silica-gel membrane to which total RNA binds. Residual DNA was digested by an on-column procedure (RNase-Free DNase; Qiagen); DNA fragments and other contaminants were removed from the column before total RNA was eluted from the column with 30 μl RNase-free water. For each sample, first-strand cDNA was synthesized from 2.5 μg total mRNA using Superscript III First-Strand Synthesis System SuperMix (Invitrogen); the mixture was incubated at 65°C for 15 min, chilled on ice for 1 min, incubated at 50°C for 50 min and finally incubated at 70°C for 15 min to terminate the reaction. A 5-μl aliquot of each cDNA sample was amplified by RT-PCR using the forward and reverse primers against known sequences of Hsp70 genes in other shark species (see below). The PCR reaction protocol was initiated with a 5-min denaturation at 95°C and followed by 35 cycles of 95°C for 40 s, 56°C for 40 s, 72°C for 40 s; the reaction was terminated with a 7-min incubation at 72°C. A 14-μl aliquot of each PCR product from a given experiment was electrophoresed on a 1.5%-agarose gel, along with a DNA ladder (0.5 μg, 100–1000 bp, GeneRuler; Fermentas, Hanover, MD, USA). The gel was stained with ethidium bromide to visualize bands of nucleic acids separated from each experimental sample and the DNA ladder. Intensity and area of each band were analyzed and compared using NIH Image.

Primers against Hsp70 were designed using the PrimerPremier Program (Premier Biosoft, Palo Alto, CA, USA). Primer design was based on the known Hsp70 gene sequences from 12 other shark species (species and GenBank accession numbers: *Alopias superciliosus*, AF502451; *Alopias vulpinus*, AF502457; *Cetorhinus maximus*, AF502489; *Mitsukurina owstoni*, AF502477; *Isurus oxyrinchus*, AF502522; *Lamna ditropis*, AF502462; *Megachasma pelagios*, AF502470; *Odontaspis ferox*, AF502442; *Pseudocarcharias kamoharai*, AF502484; *Carcharias taurus*, AF502436; *Carcharodon carcharias*, AF502529; *Alopias pelagicus*, AF502445). The forward and reverse primers were 5′-AGCCCAAGGTGAAGGTC-3′ and 5′-TGGTGATGGAG-GTGTAAAA-3′ and the anticipated product size was 597 bp. The predicted range for the ideal annealing temperature was 50–56°C. To test the efficacy of these primers at various annealing temperatures, cDNA was generated from total RNA extracted from representative heat-stressed isolated lateral CP (1-h incubation at 23.5°C followed by 1.5-h incubation at 13.5°C) and amplified by RT-PCR protocols incorporating annealing temperatures of 50°C, 52°C, 54°C and 56°C. Aliquots of the PCR products generated at these respective annealing temperatures were electrophoresed on a single 1.5% agarose gel, and the area, intensity and clarity of each nucleic acid band were integrated and compared (NIH Image). The annealing temperature of 56°C yielded the greatest amount of product with minimal contamination and was utilized in the PCR protocol for comparison of relative levels of Hsp70 mRNA under various experimental conditions. The PCR product was sequenced by the Mount Desert Island Biological Laboratory DNA Sequencing Center. The sequence was
CAGGTNNGANAACCTTCTCCCCGAGGAATCTCTTCC-ATGGTGCTGACCAAGATGAAGGAAACGGCCGAGGC-TTACCTGGGCCACACCGTCACCAACGCTGTTATCAC-TGTGCCCGCTTACTTCAATGACTCCCAGCGCCAGGC-AACCAAAGACGCTGGTGTGATCGCTGGTCTCACTGT-CCTGCGTGTCATCAATGAGCCGACGGCNGCTGCCAT-TGCCTACGGNCTATACAAGAAGGGCANAGGTGAGC-ACAATGTTCTCATCTTTGACTTGNGTGGTGGTACCTT-CNACGTCTCTATTCTCACCATTGACNACGGTATCTTT-NANGTGAAATCNACNGNTGGTGACACCCACTTGGGA-NGAGAGGACTTTGATAATCNCNTGGNCANTCNCTTC-ATTGAGGANTTCAAGCGTAAATACAAGAAGGACAT-CAGTCATAACAANANGGCNGNCAGGANGCTGAGGA-CAGCCTGCGAGAGANCAAANAGAACCNTGTCTTCCA-GCACCCNAGNNNNTATNGAGATTGACTNTCTGNTTG-AAGGCATAGACTTTTACCCCTCCATCNCCAAA
(GenBank accession number DQ913093). This segment of the *S. acanthias* Hsp70 gene was 86–88% identical to Hsp70 gene sequences previously submitted for 12 other shark species. Homology to rat and human Hsp70 genes was 84% and 79%, respectively.

Electron microscopy

After experimental treatments, segments of IVth CP (~60 mg wet mass) were fixed with 1.5% glutaraldehyde and 1.5% formaldehyde in a high sucrose-cacodylate buffer

(150 mmol l^{-1} sodium cacodylate, 3 mmol l^{-1} $MgCl_2$ and 20% sucrose, pH 7.4) on ice for 2 h as described previously (Villalobos et al., 2002). Tissues were rinsed in chilled buffer and stored overnight at 4°C, post-fixed with 1% glutaraldehyde and 2% osmium tetroxide and processed for scanning or transmission electron microscopy. Details were reported previously (Villalobos et al., 2002).

Chemicals

TMAO, urea, zinc sulfate, unlabeled 2,4-D, probenecid and 2,4,5-T were purchased from Sigma-Aldrich. KNK437 (Heat Shock Protein Inhibitor I, *N*-formyl-3,4-methylenedioxy-benzylidene-γ-butrolactam) was purchased from Calbiochem (La Jolla, CA, USA). [^{14}C]2,4-D (1.85×10^9 Bq mmol l^{-1}) was purchased from American Radiolabeled Chemical, Inc. (St Louis, MO, USA) or Moravek (Brea, CA, USA). All other chemicals were of the highest grade and obtained from commercial vendors.

Statistics

Data are presented as means ± standard error (s.e.m.). For 2,4-D transepithelial flux experiments, control and experimental 60-min fluxes or treatment-sensitive components were compared by one-tailed Student's paired *t*-test. Differences were deemed significant at $P\leqslant0.05$.

Results

Heat-induced modulation of transport of 2,4-D and Hsp70 accumulation

Tissues used for heat stress studies were temperature acclimated in explant culture for 48–72 h (referred to henceforth as 48-h-explants) prior to flux measurements in an attempt to reduce the possible effects of variable *in vivo* stress that might result from capture and handling. Prior work had shown that 2 h were adequate to allow the stress regimen to maximally induce synthesis and accumulation of hsps in various tissues of other fishes (Brown et al., 1992; Mosser et al., 1986). Our stress treatments included time for adequate synthetic activity, and, thus, the earliest time for tissue assessment was 7.5 h post-treatment in culture medium (13.5°C, referred to as 7.5-h-explants), at which time the Hsp70:actin pixel density ratio had stabilized at 1.31±0.17 and was no different in 48-h-explants (1.42±0.05). Freshly isolated tissues had an R_t of 87±17 Ω cm^2, which was not significantly different from that of 7.5-h-explants (Table 1). However, there was a 3-fold decrease in mean R_t of IVth CP to ~25 Ω cm^2 in 48-h-explants (Table 1). The presence or absence of TMAO in the culture medium had no effect on this change. The R_t in either medium was also unaffected by zinc or heat stress treatments. Similar incubation in the presence of 0.2% DMSO, however, significantly lowered the R_t of 7.5-h-explants (Table 1).

Exposure of 48-h-explants to an acute temperature elevation of 5°C for 6 h followed by a 1.5 h recovery had no significant effect on transport with or without TMAO (Fig. 2). Acutely increasing the incubation temperature by 10°C for 1 h (henceforth referred to as heat stress) with a 1.5-h recovery at 13.5°C caused a significant decrease in net active transport of 2,4-D from the CSF to blood in the presence of TMAO. However, in the absence of TMAO (isosmotic replacement with urea), active flux was unchanged by heat stress (Fig. 2). The tabulated unidirectional fluxes shown in Fig. 2 indicate that heat stress in the presence of TMAO caused the tissues to become 'leaky', i.e. transepithelial 2,4-D flux increased in both directions.

The preservation of transport with heat stress in the absence of the osmolyte was associated with greater accumulation of Hsp70. Experimental treatments to test for the effects of TMAO on stress-induced modulation of Hsp70 paralleled those implemented to investigate the effects of TMAO on stress-induced modulation of 2,4-D transport. In non-heated tissues held continuously for 48–72 h at 13.5°C, accumulation of Hsp70 in the absence of TMAO was comparable to that in the presence of TMAO (Fig. 3). In heat stressed tissues, Hsp70:actin ratios in TMAO-free conditions were, on average, 2-fold greater than the ratios in tissue heat-stressed in the presence of TMAO. Thus, the increased accumulation of Hsp70 was coincident with the tissue-level resistance of the organic anion transport machinery to heat stress.

Table 1. *Transepithelial electrical resistances (R_t) of dogfish shark choroid plexuses upon exposure to thermal or zinc stresses in the presence or absence of TMAO, dimethyl sulfoxide or KNK437*

	R_t (Ω cm^2)	
	No TMAO	TMAO
48-h-explants		
Control	22±3.9 (6)	16±3.9 (6)
Heat stress	32±5.1 (6)	28±3.9 (6)
7.5-h-explants*		
Zinc-Free	71±7.1 (5)	72±13.1 (6)
50 μmol l^{-1} zinc	62±11.1 (5)	70±18.7 (6)
	DMSO	KNK437
No TMAO-7.5-h-explants**		
Control	37±5.0 (7)	33±8.7 (7)
50 μmol l^{-1} zinc	39±6.1 (8)	25±5.6 (8)***

Values are means ± s.e.m. (*N*) following 90 min in Ussing Chambers. 7.5-h-Explants were assayed 7.5 h after removal from the animal; 48-h-explants were maintained for 48–72 h in culture medium at 13.5°C. Heat stress was elevation of bath temperature +10°C to 23.5°C for 1 h followed by 1.5-h recovery at control temperature (13.5°C). Zinc exposure was 6 h followed by 1.5-h recovery in zinc-free medium.

*7.5-h-Explants had significantly higher R_t than 48-h-explants at $P<0.05$. Dimethyl sulfoxide (DMSO) was used at 0.2% as vehicle for 100 μmol l^{-1} KNK437.

**All tissues in DMSO had significantly lower R_t than 7.5-h-explants without DMSO at $P<0.05$.

***R_t was significantly lower in tissues treated with zinc plus KNK437 as compared to zinc plus DMSO at $P<0.04$.

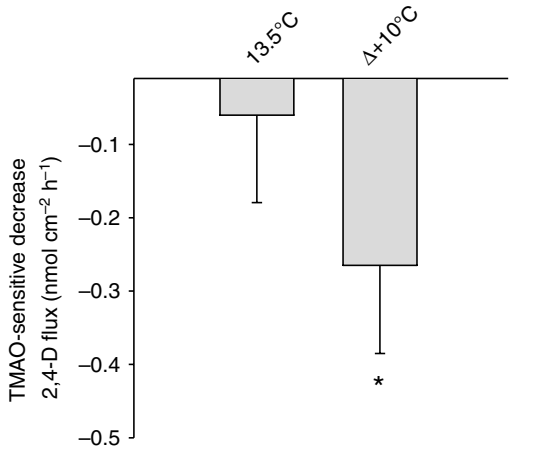

	Mean flux (nmol cm^{-2} h^{-1})		
	B to C	C to B	Net
Control + TMAO	0.5±0.26	−0.8±0.30	−0.3±0.11
Control – TMAO	0.3±0.06	−0.7±0.15	−0.4±0.16
Δ+5°C + TMAO	0.3±0.07	−0.6±0.02	−0.3±0.07
Δ+5°C – TMAO	0.3±0.22	−0.6±0.28	−0.2±0.15
Δ+10°C + TMAO	0.9±0.46*	−0.9±0.38	−0.1±0.11*
Δ+10°C – TMAO	0.1±0.08	−0.5±0.10	−0.4±0.10

Fig. 2. Trimethylamine oxide (TMAO)-sensitivity of heat-induced change in net active cerebrospinal fluid-to-blood (CSF-to-blood) [^{14}C]2,4-dichlorophenoxyacetic acid (2,4-D) fluxes across paired halves of shark IVth choroid plexus following 48 h in explant culture. Fluxes of 2,4-D were determined after tissues were exposed, ± 72 mmol l^{-1} TMAO, to treatment as follows. Control, 7.5 h at 13.5°C; Δ+5°C heat stress, 18.5°C for 6 h plus recovery at 13.5°C for 1.5 h; Δ+10°C heat stress, 5 h at 13.5°C then 1 h at 23.5°C followed by recovery at 13.5°C for 1.5 h. Tabulated data show the mean unidirectional fluxes from which net data were derived. B to C, blood-to-CSF flux; C to B, CSF-to-blood flux. Data are means ± s.e.m. (*N*=6). *Significant effect of TMAO at *P*<0.05.

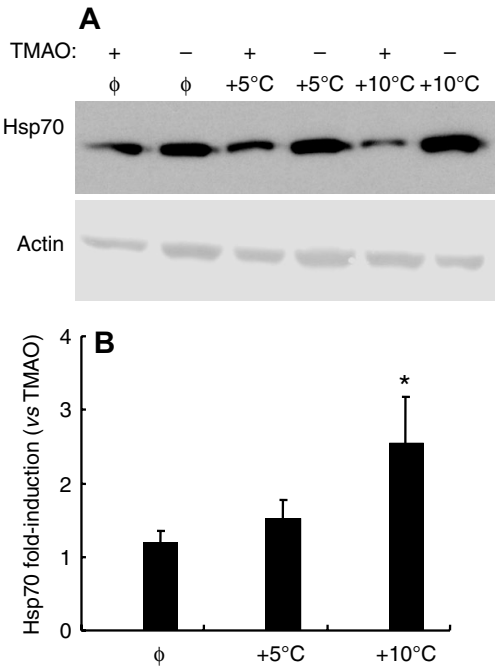

Fig. 3. Heat shock protein (hsp) accumulation in explanted shark lateral choroid plexus (CP) after thermal stress in the presence and absence of trimethylamine oxide (TMAO). Lateral CPs from individual sharks were each divided into three equal-sized segments, totaling six pieces; tissues were separated into three pairs and incubated, ± 72 mmol l^{-1} TMAO, at 13.5°C for 7.5 h (ϕ), at 18.5°C for 6 h plus recovery at 13.5°C for 1.5 h (+5°C), or 23.5°C for 1 h plus recovery at 13.5°C for 1.5 h (+10°C). (A) Representative immunoblot for Hsp70 and actin accumulation in lysates of non-heated and heat-stressed lateral CP. (B) Graphical summation of Hsp70 accumulation (normalized to actin accumulation) in non-heated and heat-stressed lateral CP (means ± s.e.m., *N*=4). For each condition, fold-induction of heat shock protein was calculated by dividing the normalized Hsp70 accumulation in the absence of TMAO by the normalized Hsp70 accumulation in the presence of TMAO. *Significantly different from paired tissue treated in the presence of TMAO at *P*<0.05.

Zinc-induced modulation of transport of 2,4-D and Hsp70 accumulation

IVth CP tissues were incubated for 6 h (13.5°C) with or without 50 μmol l^{-1} $ZnCl_2$ with TMAO or without TMAO; all tissues were then rinsed and incubated for an additional 1.5-h recovery in zinc-free medium containing TMAO. Irrespective of the presence of TMAO, R_t was not altered by zinc exposure (Table 1). However, zinc exposure in the absence of TMAO markedly increased net 2,4-D transport from the CSF side to the blood side (Fig. 4); active transport increased by an average of ~40%. By contrast, zinc exposure in the presence of TMAO had no effect on transport. The zinc-induced increase in net active transport appeared to be due mostly to an increase in the unidirectional CSF-to-blood flux; there was little change in blood-to-CSF flux.

Induction of Hsp70 in CP exposed *in vitro* to zinc in the presence and absence of TMAO is shown in Fig. 5. In both the presence and absence of TMAO, zinc exposure induced increased accumulation of Hsp70. In tissues incubated with TMAO, zinc increased the accumulation of Hsp70 by 1.36-fold as compared to levels of the protein in tissues not exposed to zinc. However, in tissues incubated without TMAO, zinc exposure increased accumulation of Hsp70 by 2.65-fold as compared to levels of stress protein in TMAO-free tissues not treated with zinc. Furthermore, the pixel density ratio of Hsp70 to that of actin in tissues exposed to zinc in the absence of TMAO was roughly 2-fold greater than the ratio in tissues exposed to the metal in the presence of the osmolyte. Thus, although zinc induced accumulation of Hsp70 in the presence of TMAO, induction of Hsp70 was far more pronounced in the absence of TMAO. The increased level of Hsp70 accumulation was, thus, associated with increased OA transport rate.

The apparent correlation of increased active OA transport by CP and the cellular stress response was further examined with the novel inhibitor of acquisition of thermotolerance and heat shock protein induction, KNK437 (Yokota et al., 2000). Because zinc was a strong inducer in the absence of TMAO,

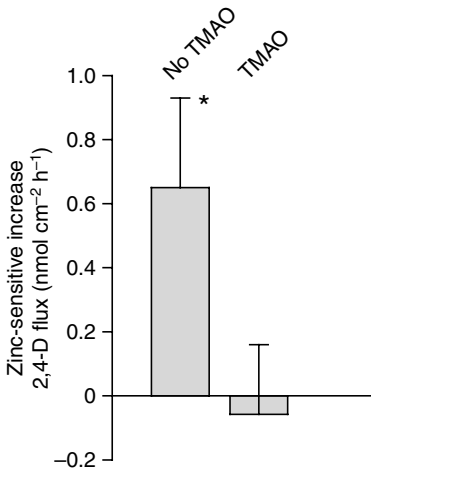

	Mean flux (nmol cm^{-2} h^{-1})		
	B to C	C to B	Net
Control + TMAO	0.6±0.13	–2.6±0.52	–2.0±0.43
Zinc + TMAO	0.5±0.12	–2.3±0.35	–1.8±0.40
Control – TMAO	0.6±0.17	–1.7±0.21	–1.1±0.36
Zinc – TMAO	0.8±0.25	–2.6±0.37	–1.8±0.26*

Fig. 4. Trimethylamine oxide (TMAO)-sensitivity of zinc-induced change in active cerebrospinal fluid-to-blood (CSF-to-blood) [^{14}C]2,4-dichlorophenoxyacetic acid (2,4-D) fluxes across paired halves of shark IVth choroid plexus. Fluxes of 2,4-D were determined after tissues were exposed, ± 72 mmol l^{-1} TMAO (13.5°C), to treatment as follows. Control, 6h in zinc-free medium + 1.5 h recovery in L-15E; Zinc-treated, 6 h in 50 μmol l^{-1} $ZnSO_4$ + 1.5 h recovery in L-15E. Tabulated data show the mean unidirectional fluxes from which net data were derived; B to C, blood-to-CSF flux; C to B, CSF-to-blood flux. Data are means ± s.e.m. (*N*=6). *Significant effect of zinc at *P*<0.05.

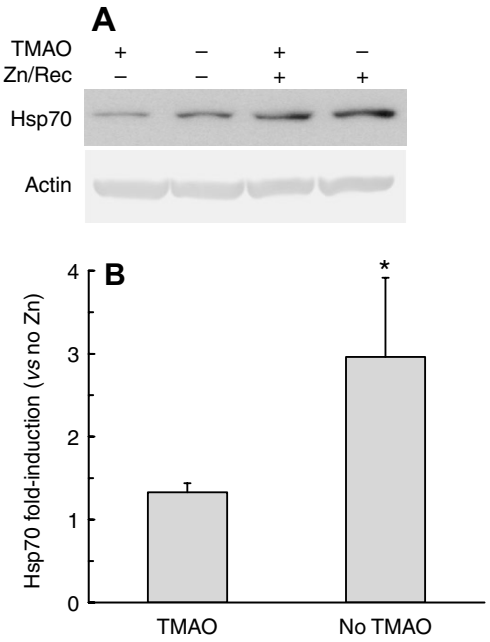

Fig. 5. Heat shock protein accumulation in isolated shark lateral choroid plexus (CP) after zinc exposure in the presence and absence of TMAO. Each lateral CP from an individual shark was divided in half yielding four segments. Paired tissue segments were incubated, ± 72 mmol l^{-1} TMAO (13.5°C), with 0 or 50 μmol l^{-1} $ZnSO_4$ for 6 h; all tissues were then incubated in zinc-free medium with TMAO for 1.5 h. (A) Representative immunoblot for Hsp70 and actin accumulation in lysates of zinc-free and zinc-exposed lateral CP. (B) Graphical summation of Hsp70 induction by zinc ± TMAO in lateral CP. Hsp70 accumulation was normalized to that of actin. For zinc exposure with TMAO, fold-induction of Hsp70 was calculated by dividing the normalized Hsp70 accumulation in zinc-treated tissue by that in non-exposed timed-control tissue incubated with TMAO. Likewise, for zinc exposure without TMAO, fold-induction of Hsp70 was calculated by dividing Hsp70 accumulation in zinc-treated tissue by that in non-exposed timed-control tissue incubated without TMAO (means ± s.e.m., *N*=4; *P<0.05 *vs* fold-induction with TMAO).

we repeated the flux experiments above with and without 100 μmol l^{-1} KNK437. Tissues were preincubated with inhibitor for 30 min prior to exposure to 50 μmol l^{-1} zinc + KNK437 and no TMAO for 6 h followed by 1.5 h recovery in normal L-15E with KNK437. Zinc-exposed controls were treated identically except with vehicle only (0.2% DMSO). As shown in Fig. 6, the stimulatory effect of zinc in the absence of TMAO was completely blocked by KNK437. Net active flux was reduced about 7-fold. Some non-specific damage may have occurred with combined zinc and KNK437 exposure, as indicated by the significantly lowered R_t in the latter (Table 1). In a separate set of tissues, referred to as controls in Fig. 6, the hsp inhibitor also strongly inhibited transport in the absence of zinc stimulation (Fig. 6), although not to the same extent. Fig. 7 shows that KNK437 treatment was effective in reducing hsp production in tissues exposed to zinc in the absence of TMAO. As compared to time-matched control tissues (no zinc), zinc exposure with recovery increased Hsp70 accumulation by 4.09-fold; in the presence of KNK437, the hsp was induced by 1.45-fold (*N*=4). As displayed in the immunoblot shown in Fig. 7, KNK437 also reduced Hsp70 expression in non-zinc exposed tissues about 3-fold. In addition, as compared to Hsp70 accumulation in CP tissue collected directly from the shark, 7.5-h-explant culture at 13.5°C without TMAO increased Hsp70 accumulation by 2.02-fold. Thus, alterations of OA transport in both zinc-exposed and control 7.5 h-explanted cultures was associated with relative Hsp70 accumulation.

Stress-induced transcription of Hsp70 mRNA

Transcription of the Hsp70 gene was evaluated in CP subjected *in vitro* to +10°C heat stress or zinc exposure in the presence or absence of TMAO; expression levels of Hsp70 mRNA were analyzed by semi-quantitative RT-PCR (Fig. 8). For each individual heat stress or zinc exposure experiment, paired, equal-sized fragments of CP from a single shark were used. To investigate the influence of TMAO on heat-induced changes in Hsp70 mRNA expression, levels of Hsp70 mRNA were compared among tissues held at 13.5°C incubated in both the presence and absence of TMAO and tissues heat stressed in the presence and absence of the osmolyte (23.5°C for 1 h

followed by 1.5 h at 13.5°C). In the non-heat stressed condition, the relative level of Hsp70 mRNA in the absence of TMAO was nearly twice that in the presence of TMAO (1.98±0.13; *N*=3). Heat stress increased expression of Hsp70 mRNA irrespective of the presence of TMAO. However, the relative levels of Hsp70 mRNA in the absence of TMAO were approximately 2-fold greater than levels in the presence of TMAO (2.24±0.98; *N*=3).

The effects of zinc exposure on Hsp70 mRNA expression were examined in a separate series of tissues. Under zinc-free conditions (13.5°C, 7.5 h), relative levels of Hsp70 mRNA in tissue incubated without TMAO were roughly 50% greater than levels in tissue incubated with TMAO (1.57±0.01). With zinc exposure, there were modest increases in Hsp70 mRNA in both the presence and absence of TMAO. Nevertheless, the ratio of the level of Hsp70 mRNA in the absence of TMAO to the level of Hsp70 mRNA in the presence of TMAO was 1.66±0.19. Thus, although heat stress and zinc exposure induced increases in expression of Hsp70 mRNA in the presence of TMAO, both basal and stress-induced expression of heat shock protein mRNA were greater in the absence of the osmolyte.

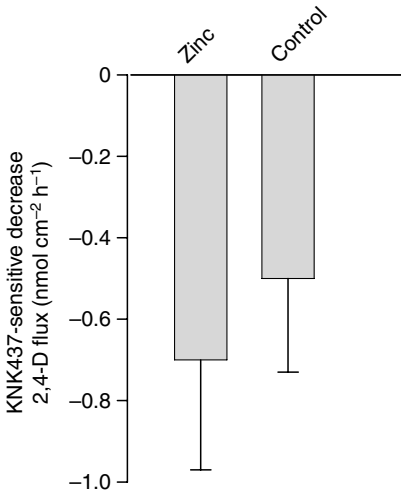

	Mean flux (nmol cm^{-2} h^{-1})		
	B to C	C to B	Net
Zn Control – TMAO	2.2±0.47	–3.6±0.58	–1.4±0.28
Zn + KNK – TMAO	0.6±0.07	–0.8±0.09	–0.2±0.06*
Control – TMAO	1.5±0.27	–3.1±0.37	–1.7±0.30
KNK – TMAO	1.6±0.61	–2.7±0.97	–1.1±0.37*

Fig. 6. KNK437-sensitivity of zinc-induced change in active cerebrospinal fluid-to-blood (CSF-to-blood) [^{14}C]2,4-dichlorophenoxyacetic acid (2,4-D) fluxes across paired halves of shark IVth choroid plexus in the absence of trimethylamine oxide (TMAO). Fluxes of 2,4-D were determined after tissues were exposed at 13.5°C, ± 100 μmol l^{-1} KNK437 (vehicle control was 0.2% DMSO), to treatment as follows. Zinc-treated, 6 h in 50 μmol l^{-1} $ZnSO_4$ + 1.5 h recovery in L-15E (*N*=8); Control, 6 h in zinc-free medium + 1.5 h recovery in L-15E (*N*=7). Tabulated data show the mean unidirectional fluxes from which net data were derived. B to C, blood-to-CSF flux; C to B, CSF-to-blood flux. Data are means ± s.e.m.; *P<0.05 *vs* net flux in paired tissue treated without KNK437.

CP ventricular surface morphology and ultrastructure following thermal stress and zinc exposure

The CSF-facing surface topology and ultrastructural morphology of isolated CP are shown in Fig. 9. As viewed by transmission electron microscopy, CP is comprised of an epithelial monolayer rich in mitochondria with densely packed apical microvilli that interface with the CSF *in vivo* and an interdigitated basolateral membrane that interfaces with the

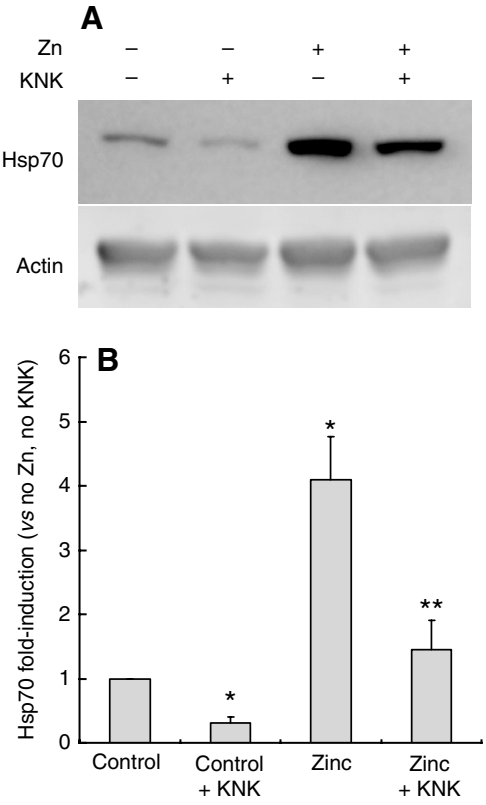

Fig. 7. Heat shock protein accumulation in isolated shark lateral choroid plexus (CP) after zinc exposure with KNK437 in absence of trimethylamine oxide (TMAO). Lateral CPs from an individual shark were divided, yielding four equal-sized segments; each segment was incubated at 13.5°C in TMAO-free L15E medium. Tissues were incubated without zinc ± 100 μmol l^{-1} KNK437 or with 50 μmol l^{-1} $ZnSO_4$ ± 100 μmol l^{-1} KNK437 for 6 h; all tissues were then incubated for 1.5 h in zinc-free medium containing TMAO ± 100 μmol l^{-1} KNK437. For tissues not treated with KNK437, medium contained 0.2% DMSO (vehicle). (A) Representative immunoblot analysis of Hsp70 and actin accumulation in lysates of lateral CP treated in the absence of TMAO without zinc or with zinc ± KNK437. (B) Graphical comparison of Hsp70 induction by zinc exposure ± KNK437 in the absence of TMAO (mean ± s.e.m.; *N*=3). Fold-induction of Hsp70 was calculated by dividing Hsp70 accumulation (normalized to actin) in zinc-treated tissue without or with KNK437 by the normalized Hsp70 accumulation in timed-control tissue incubated without KNK437. *P<0.05 *vs* fold-induction in control and **P<0.05 *vs* fold-induction in zinc only, respectively.

interstitial compartment and a discontinuous layer of adipocytes (the large fat globules can be seen in Fig. 9F,H,I). As the capillaries within the stroma are fenestrated, the 'blood' compartment is functionally continuous with the interstitial compartment. The tight junctions between the epithelial cells form the blood–CSF barrier and appeared to remain intact under all conditions tested. As viewed by scanning electron microscopy, the apical microvilli are clavate or club-shaped rather than filiform (Fig. 9A). The differences in the ultrastructure and ventricular surface morphology of IVth CP fixed immediately upon removal from the animal (referred to as *in vivo*) compared with non-stressed CP at 7.5 h in L-15E (13.5°C) were slight (Fig. 9A,F and Fig. 9B,G). Although microvillus length was greater in 7.5-h-explants (1.77±0.12 μm *vs* 1.17±0.03 μm; $P<0.05$), there was no difference in size and shape of the clavate tip of the microvilli (maximum traverse width: *in vivo*, 0.30±0.03 μm; non-stressed explanted tissue, 0.33±0.05 μm; minimum transverse width: non-stressed, 0.09±0.005 μm; *in vivo*, 0.07±0.008 μm). Replacement of TMAO with equimolar mannitol in the L-15E had no effect on morphology (data not shown).

Morphological comparisons were made after a 5°C heat stress (18.5°C for 6 h plus recovery at 13.5°C for 1.5 h), a 10°C heat stress (23.5°C for 1 h plus recovery at 13.5°C for 1.5 h) and zinc exposure at 13.5°C (50 μmol l^{-1} $ZnSO_4$ for 6 h plus recovery in zinc-free medium for 1.5 h). Transmission electron micrographs indicated that heat stress and zinc treatment caused no detachment of epithelium from the basement membrane or any remarkable changes in vascular elements; tight junctions also remained intact under each stress condition. The mean length of the microvilli in stressed explanted tissue was comparable to that in non-stressed explanted tissue (Δ+5°C, 1.12±0.04 μm; Δ+10°C, 1.62±0.08 μm; Zn, 1.82±0.11 μm). However, a profound morphological change was the expansion of the tips of the microvilli in both thermally stressed and zinc-treated tissues. Δ+5°C with recovery resulted in expansion of the microvilli tips in the maximum and minimum transverse dimensions to 0.88±0.096 μm and 0.22±0.03 μm, respectively; Δ+10°C induced even greater and more irregular expansion to 1.28±0.08 μm and 0.20±0.3 μm. Zinc treatment also expanded microvilli tips to a degree comparable to heat stress; maximum and minimum transverse dimensions were 0.96±0.095 μm and 0.25±0.04 μm, respectively. Ultrastructurally, these expanded microvilli appeared to be multiple layers and myeloid-like whorls of plasma membrane; this was particularly noteworthy with Δ+10°C.

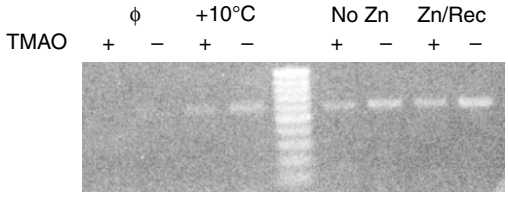

Fig. 8. Expression of Hsp70 mRNA in isolated lateral choroid plexus (CP) following +10°C heat shock or zinc exposure in the presence and absence of trimethylamine oxide (TMAO). Levels of Hsp70 mRNA were compared in non-treated and stressed lateral CP tissues obtained from the same shark. +10°C heat stress: tissue segments were incubated in medium with and without TMAO at 13.5°C for 7.5 h (ϕ) or at 23.5°C for 1 h then 13.5°C for 1.5 h (+10°C). Zinc exposure/recovery: tissue segments were incubated at 13.5°C in medium with and without TMAO for 7.5 h without zinc (No Zn) or with 50 μmol l^{-1} $ZnSO_4$ for 6 h then without zinc for an additional 1.5 h (Zn/Rec). Relative levels of hsp70 mRNA in non-treated and stressed tissues were analyzed by semi-quantitative RT-PCR. Shown here is an EtBr-stained 1.5% agarose gel on which aliquots of PCR products from representative sets of heat-stressed and zinc-exposed tissue, along with a DNA ladder, were electrophoresed; N=2–3 for each experiment.

Discussion

Whereas the cellular stress response is well known to increase cell survival in the face of subsequent physicochemical stress, its influence on functional integrity at the tissue level has been less frequently reported. Several studies indicate that a conditioning stress, i.e. a stress sufficient to induce increased synthesis and accumulation of hsps, can protect the differentiated tissue-level function of transepithelial transport (Brown et al., 1992; Hightower et al., 2000; Ikari et al., 2002; Renfro et al., 1993; Kultz, 2005). Hsp70 is among the battery of stress responsive proteins that comprise what Kultz has called the minimal stress proteome (Kultz, 2005). Thus, inducible Hsp70 is a good indicator of a generalized cell stress response that includes protein stabilization, DNA repair and free radical scavenging. The present study of isolated dogfish shark CP showed that non-lethal physicochemical stressors, such as excessive heat and heavy metal exposure, not only induced Hsp70 production by shark CP but significantly impacted the capacity of CP to actively remove OAs from CSF. Notably, however, this brain barrier's functional response to cellular stress was significantly impeded by a physiological level of TMAO.

Without application of the aforementioned stresses, the presence or absence of TMAO during explant culture of shark IVth CP had no effect on net 2,4-D absorption. However, a +10°C heat stress in the *presence* of TMAO was clearly more damaging to transepithelial transport than in the *absence* of TMAO. Not only was net active transport decreased, but passive leak flux was increased. The unchanged R_t indicated that the latter was not due to a loss of tight junction integrity, a phenomenon not without precedent that may be due to redistribution of transporters caused by transient changes in cytoskeletal elements (Brown et al., 1992). Transmission electron microscopy revealed pronounced and irregular expansion of microvilli and melding of plasma membrane at the apical pole of the epithelium in Δ+10°C stressed tissues; however, there was no sloughing of cells, detachment from the basement membrane or opening of junctional complexes. Nevertheless, in the absence of broad destructive changes in

morphology, Δ+10°C heat stress in the presence of TMAO markedly decreased OA transport. By comparison, transepithelial transport seemed unaffected by the substantial temperature shift when TMAO was not present in the incubation medium. Similarly, net active OA transport was greater in CP exposed to 50 μmol l^{-1} zinc without TMAO, and the lower transport capacity in TMAO-supplemented tissues could not be attributed to differences in either R_t or leak flux. This lack of change in, or apparent protection of, transport in TMAO-deprived CP tissues was associated with considerably higher levels of Hsp70. The suppression of Hsp70 induction by TMAO was consistent with work on the Madin-Darby canine kidney cell line (MDCK) that showed the stabilizing osmolyte betaine strongly attenuated the stimulation of increased Hsp70 mRNA by a denaturing level of hypertonicity and by elevated temperature (Sheikh-Hamad et al., 1994). The effect was attributed to greater stabilization of proteins in the presence of a high concentration (250 mmol l^{-1}) of osmolyte and, as a consequence, attenuated protein denaturation, thereby decreasing the signal for increased synthesis of stress proteins (Hightower, 1980; Ananthan et al., 1986; Hightower, 1991). In shark CP, the putative protein stabilizing effect of TMAO was manifested in the suppression of Hsp70 production. Support for the TMAO effect was seen in the effects of the heat shock protein inhibitor KNK437. The latter coincidentally blocked Hsp70 accumulation and drastically lowered active OA transport. Interestingly, this effect was also seen in control, explanted tissues, revealing stress-induced changes brought about by the *in vitro* environment.

Proposed mechanisms of cytoprotection usually indicate that it is the prevention of damage to macromolecules or the facilitation of their repair by chaperone proteins or chemical cytoprotectants that promotes cell survival. However, in functional transporting epithelia, an associated stress-induced increase in transepithelial transport capacity has been observed that may either compensate for lost capacity due to damage or actually increase total capacity (Hightower et al., 2000). Preconditioning of both flounder and porcine cultured renal proximal tubule with mild heat-stress (i.e. +5°C above baseline with recovery), which produced pronounced induction of Hsp70 protein in those tissues, prevented attenuation of transepithelial transport of glucose and sulfate by severe heat shock (+10°C above baseline with recovery) that was otherwise observed in naïve tissues (Renfro et al., 1993; Sussman and Renfro, 1997). In flounder proximal tubule, a preconditioning zinc exposure sufficient to induce synthesis and accumulation of Hsp70 also elicited an increase in the tissue's capacity to transport sulfate, an effect that may

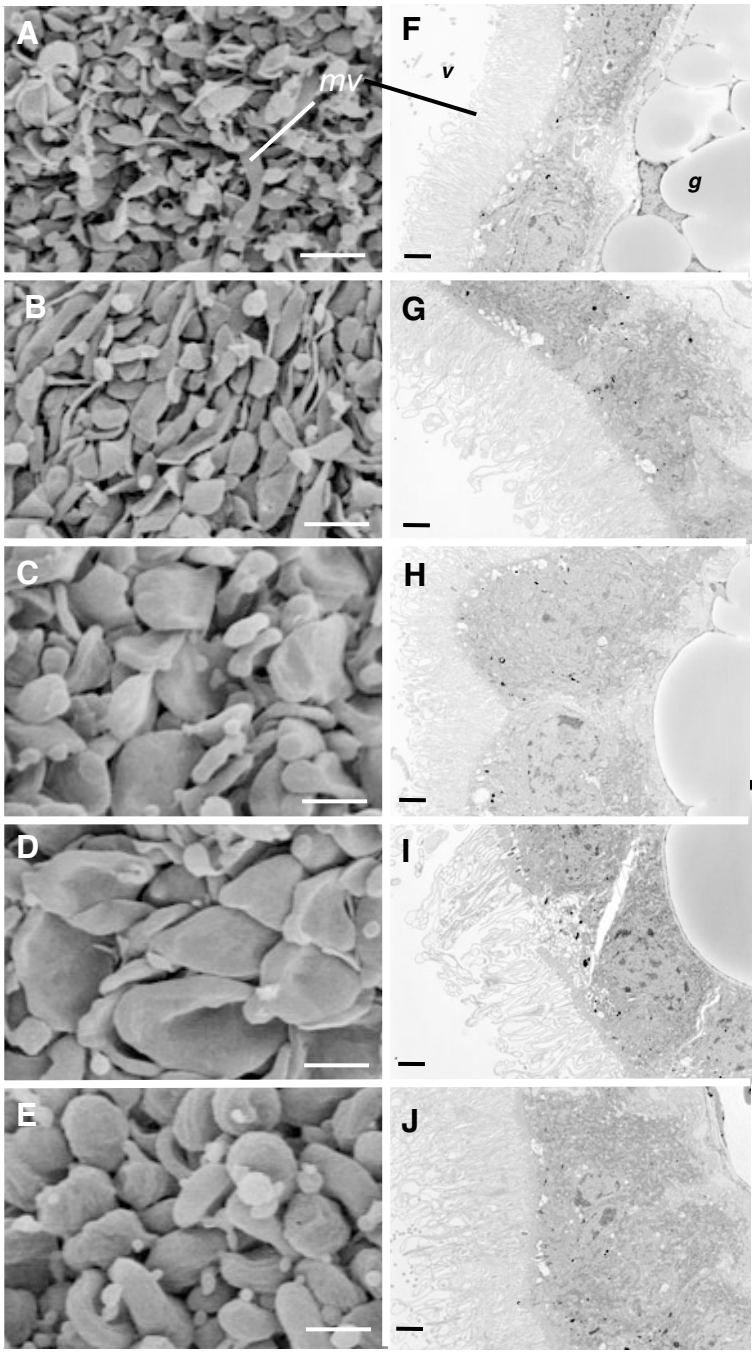

Fig. 9. Electron micrographs of isolated shark choroid plexus (CP) subjected *in vitro* to heat stress or zinc exposure in complete culture medium (L-15E). (A–E) Scanning electron micrographs of dogfish shark IVth CP ventricular surface (CSF-side); (F–J) transmission electron micrographs of shark IVth CP. (A,F) Freshly harvested tissue immediately processed for fixation. (B,G) Tissues held at 13.5°C for 7.5 h in L-15E. (C,H) Tissues incubated at 18.5°C for 6 h followed by incubation at 13.5°C for 1.5 h. (D,I) Tissues incubated initially at 13.5°C for 5 h, then at 23.5°C for 1 h followed by 13.5°C for 1.5 h. (E,J) Tissues incubated with 50 μmol l^{-1} $ZnSO_4$ at 13.5°C for 6 h followed by recovery in zinc-free medium at 13.5°C for 1.5 h. mv, microvilli; v, ventricular or cerebrospinal fluid-side; g, fat globule. Scale bars, 5 μm.

contribute to the apparent protection of sulfate transport against both severe heat shock and chemical intoxication (Renfro et al., 1993). Inhibition of hsp synthesis or gene transcription prevented the effectiveness of stress preconditioning in protection of solute transport. In the present study, exposure of shark CP to 50 μmol l^{-1} zinc elicited a very strong cellular stress response as judged by Hsp70 accumulation. Although zinc is a vital nutrient, essential for growth, development and reproduction in all organisms and present in at least 300 enzymes including all six IUBMB classes (Laity et al., 2001), it also adversely influences the quaternary structure of many proteins. Thus, cells very efficiently regulate total and free concentrations of intracellular zinc *via* coordinated regulation of the influx and efflux of the metal with its binding to metallothionein (Cousins et al., 2006; Liuzzi and Cousins, 2004; Tapiero and Tew, 2003). The stress response noted in the present study indicated significant overload of those mechanisms in the CP. The stimulation of cellular or integrative tissue function to levels higher than those in unexposed controls by a chemical denaturant has been frequently reported and is a manifestation of hormesis (Bukowski and Lewis, 2000; Calabrese, 2005; Rattan, 2004). Thus, the stimulation by zinc exposure of herbicide transport from CSF to blood compartments in isolated CP to levels above that of unexposed tissues is consistent with hormesis associated with the cellular stress response. This phenomenon has been previously observed in renal proximal tubule (Renfro et al., 1993).

As Somero has pointed out (Somero, 1995), both protein turnover and protein function benefit from a balance between stability and lability. Constitutive as well as stress-induced hsps prevent nonspecific protein aggregates; however, maintenance of high levels of hsps greatly increases the cellular energy requirements. Expression of inducible hsps during nonstressful periods may be detrimental to growth and lead to accumulation of useless and difficult to remove aggregates of hsps themselves (Feder et al., 1992). The suppression of hsp production during stress by TMAO, as observed in mammalian cell lines and renal medullary cells (Neuhofer et al., 2005; Neuhofer et al., 2001) and now here in a stenohaline marine elasmobranch, may be beneficial to tissues in environments with only minimal or slow physicochemical fluctuations. Thus, the necessity to counteract the protein destabilizing effects of high urea and NaCl may be better served by chemical cytoprotectants rather than by energetically expensive and continuous synthesis of new hsps. Evolutionarily, ectotherms living in widely fluctuating environments appear to have a stronger cellular stress response than those in more stable conditions (Shabtay and Arad, 2005). Thus, the comparatively stable oceanic environment and ureosmotic strategy of osmoregulation may have made chemical cytoprotectants an economical alternative stress defense for spiny dogfish; however, when extreme stresses are encountered, these animals may be less able to mount an appropriate cellular stress response and therefore may be at greater risk of excessive protein injury.

In summary, active transepithelial absorption of OAs by isolated shark CP was altered in response to thermal stress and heavy metal exposure in a manner contingent on the tissue's ability to mount a cellular stress response. Impairment of Hsp70 upregulation, by inclusion of TMAO or the HSF1 inhibitor KNK437, diminished transepithelial transport under stress conditions. Collectively, these data indicate that induction of heat shock proteins in CP may be critical for sustaining the active and selective exchange of OAs between CSF and blood compartments under conditions of physicochemical stress.

List of symbols and abbreviations

hsp	heat shock protein
CP	choroid plexus
CSF	cerebrospinal fluid
2,4-D	2,4-dichlorophenoxyacetic acid
KNK437	heat shock protein inhibitor I
OA	organic anion
R_t	transepithelial electrical resistance
TMAO	trimethylamine oxide

We gratefully acknowledge the help of Jennifer Higgins, Drs Susan Edwards and Pedro Guerreiro with analysis of Hsp70 mRNA. This work was supported by NSF-IBN-0416954, NSF-DBI-0453391, NIH-NINDS-NS39452, NIH-NIEHS-ES10439, NIH-NIEHS-P30-ES03828 and NIH-NIEHS-P30-ES01247.

References

Agashe, V. R. and Hartl, F. U. (2000). Roles of molecular chaperones in cytoplasmic protein folding. *Semin. Cell Dev. Biol.* **11**, 15-25.

American Physiological Society (2002). Guiding principles for research involving animals and human beings. *Am. J. Physiol.* **283**, R281-R283.

Ananthan, J., Goldberg, A. L. and Voellmy, R. (1986). Abnormal proteins serve as eukaryotic stress signals and trigger the activation of heat shock genes. *Science* **232**, 522-524.

Blake, M. J., Nowak, T. S. and Holbrook, N. J. (1990). In vivo hyperthermia induces expression of HSP70 mRNA in brain regions controlling the neuroendocrine response to stress. *Brain Res. Mol. Brain. Res.* **8**, 89-92.

Brown, C. R., Hong-Brown, L. Q., Biwersi, J., Verkman, A. S. and Welch, W. J. (1996). Chemical chaperones correct the mutant phenotype of the delta F508 cystic fibrosis transmembrane conductance regulator protein. *Cell Stress Chaperones* **1**, 117-125.

Brown, C. R., Hong-Brown, L. Q. and Welch, W. J. (1997). Correcting temperature-sensitive protein folding defects. *J. Clin. Invest.* **99**, 1432-1444.

Brown, I. R. (1991). Expression of heat shock genes (hsp70) in the mammalian nervous system. In *Results and Problems in Cell Differentiation: Heat Shock and Development*. Vol. 17 (ed. L. E. Hightower and L. Nover), pp. 215-229. New York: Springer-Verlag.

Brown, M. A., Upender, R. P., Hightower, L. E. and Renfro, J. L. (1992). Thermoprotection of a functional epithelium: heat stress effects on transepithelial transport by flounder renal tubule in primary monolayer culture. *Proc. Natl. Acad. Sci. USA* **89**, 3246-3250.

Bukowski, J. A. and Lewis, R. J. (2000). Hormesis and health: a little of what you fancy may be good for you. *South. Med. J.* **93**, 371-374.

Burg, M. B. and Peters, E. M. (1998). Effects of glycine betaine and glycerophosphocholine on thermal stability of ribonuclease. *Am. J. Physiol.* **274**, F762-F765.

Calabrese, E. J. (2005). Paradigm lost, paradigm found: the re-emergence of hormesis as a fundamental dose response model in the toxicological sciences. *Environ. Pollut.* **138**, 378-411.

Cousins, R. J., Liuzzi, J. P. and Lichten, L. A. (2006). Mammalian zinc transport, trafficking, and signals. *J. Biol. Chem.* **281**, 24085-24089.

Ennis, S. R. and Keep, R. F. (2006). The effects of cerebral ischemia on the rat choroid plexus. *J. Cereb. Blood Flow Metab.* **26**, 675-683.

Feder, J. H., Rossi, J. M., Solomon, J., Solomon, N. and Lindquist, S. (1992). The consequences of expressing hsp70 in *Drosophila* cells at normal temperatures. *Genes Dev.* **6**, 1402-1413.

Goldstein, L., Hartman, S. C. and Forster, R. P. (1967). On the origin of trimethylamine oxide in the spiny dogfish, *Squalus acanthias*. *Comp. Biochem. Physiol.* **21**, 719-722.

Heads, R. J., Yellon, D. M. and Latchman, D. S. (1995). Differential cytoprotection against heat stress or hypoxia following expression of specific stress protein genes in myogenic cells. *J. Mol. Cell. Cardiol.* **27**, 1669-1678.

Hightower, L. E. (1980). Cultured animal cells exposed to amino acid analogues or puromycin rapidly synthesize several polypeptides. *J. Cell. Physiol.* **102**, 407-427.

Hightower, L. E. (1991). Heat shock, stress proteins, chaperoning and proteotoxicity. *Cell* **66**, 191-197.

Hightower, L. E., Brown, M. A., Renfro, J. L., Perdrizet, G. A., Rewinski, M., Guidon, P. T., Jr, Mistry, T. and House, S. D. (2000). Tissue-level cytoprotection. *Cell Stress Chaperones* **5**, 412-414.

Ikari, A., Nakano, M., Kawano, K. and Suketa, Y. (2002). Up-regulation of sodium-dependent glucose transporter by interaction with heat shock protein 70. *J. Biol. Chem.* **277**, 33338-33343.

Johanson, C. E., Palm, D. E., Primiano, M. J., McMillan, P. N., Chan, P., Knuckey, N. W. and Stopa, E. G. (2000). Choroid plexus recovery after transient forebrain ischemia: role of growth factors and other repair mechanisms. *Cell. Mol. Neurobiol.* **20**, 197-216.

Krueger-Naug, A. M., Hopkins, D. A., Armstrong, J. N., Plumier, J. C. and Currie, R. W. (2000). Hyperthermic induction of the 27-kDa heat shock protein (Hsp27) in neuroglia and neurons of the rat central nervous system. *J. Comp. Neurol.* **428**, 495-510.

Kultz, D. (2005). Molecular and evolutionary basis of the cellular stress response. *Annu. Rev. Physiol.* **67**, 225-257.

Laity, J. H., Lee, B. M. and Wright, P. E. (2001). Zinc finger proteins: new insights into structural and functional diversity. *Curr. Opin. Struct. Biol.* **11**, 39-46.

Liuzzi, J. P. and Cousins, R. J. (2004). Mammalian zinc transporters. *Annu. Rev. Nutr.* **24**, 151-172.

Mosser, D. D., Heikkila, J. J. and Bols, N. C. (1986). Temperature ranges over which rainbow trout fibroblasts survive and synthesize heat-shock proteins. *J. Cell. Physiol.* **128**, 432-440.

Neuhofer, W., Lugmayr, K., Fraek, M.-L. and Beck, F.-X. (2001). Regulated overexpression of heat shock protein 72 protects Madin-Darby canine kidney cells from the detrimental effects of high urea concentrations. *J. Am. Soc. Nephrol.* **12**, 2565-2571.

Neuhofer, W., Fraek, M.-L., Ouyang, N. and Beck, F.-X. (2005). Differential expression of heat shock protein 27 and 70 in renal papillary collecting duct and interstitial cells–implications for urea resistance. *J. Physiol. Lond.* **564**, 715-722.

Palm, D., Knuckey, N., Guglielmo, M., Watson, P., Primiano, M. and Johanson, C. (1995). Choroid plexus electrolytes and ultrastructure following transient forebrain ischemia. *Am. J. Physiol.* **269**, R73-R79.

Palmer, H. R., Bedford, J. J., Leader, J. P. and Smith, R. A. J. (2000). ^{31}P and ^{1}H NMR studies of the effect of the counteracting osmolyte trimethylamine-N-oxide on interactions of urea with ribonuclease A. *J. Biol. Chem.* **275**, 27708-27711.

Rattan, S. I. S. (2004). Mechanisms of hormesis through mild heat stress on human cells. *Ann. N. Y. Acad. Sci.* **1019**, 554-558.

Renfro, J. L., Brown, M. A., Parker, S. L. and Hightower, L. E. (1993). Relationship of thermal and chemical tolerance to transepithelial transport by cultured flounder renal epithelium. *J. Pharmacol. Exp. Ther.* **265**, 992-1000.

Riabowol, K. T., Mizzen, L. A. and Welch, W. J. (1988). Heat shock is lethal to fibroblasts microinjected with antibodies against hsp70. *Science* **242**, 433-436.

Shabtay, A. and Arad, Z. (2005). Ectothermy and endothermy: evolutionary perspectives of thermoprotection by HSPs. *J. Exp. Biol.* **208**, 2773-2781.

Sheikh-Hamad, D., Garcia-Perez, A., Ferraris, J. D., Peters, E. M. and Burg, M. B. (1994). Induction of gene expression by heat shock versus osmotic stress. *Am. J. Physiol. Renal Physiol.* **267**, F28-F34.

Somero, G. N. (1986). From dogfish to dogs: trimethylamines protect proteins from urea. *News Physiol. Sci.* **1**, 9-12.

Somero, G. N. (1995). Proteins and temperature. *Annu. Rev. Physiol.* **57**, 43-68.

Sussman, C. R. and Renfro, J. L. (1997). Heat shock-induced protection and enhancement of Na^+-glucose cotransport by LLC-PK1 monolayers. *Am. J. Physiol.* **273**, F530-F537.

Sussman-Turner, C. and Renfro, J. L. (1995). Heat shock-stimulated transepithelial daunomycin secretion by renal proximal tubule primary cultures. *Am. J. Physiol.* **267**, F135-F144.

Tapiero, H. and Tew, K. D. (2003). Trace elements in human physiology and pathology: zinc and metallothioneins. *Biomed. Pharmacother.* **57**, 399-411.

Villalobos, A. R. A., Miller, D. S. and Renfro, J. L. (2002). Transepithelial organic anion transport by shark choroid plexus. *Am. J. Physiol. Regul. Integr. Comp. Physiol.* **282**, R1308-R1316.

Yancey, P. H. and Somero, G. N. (1979). Counteraction of urea destabilization of protein structure by methylamine osmoregulatory compounds of elasmobranch fishes. *Biochem. J.* **183**, 317-323.

Yancey, P. H. and Somero, G. N. (1980). Methylamine osmoregulatory solutes of elasmobranch fishes counteract urea inhibition of enzymes. *J. Exp. Zool.* **212**, 205-211.

Yokota, S., Kitahara, M. and Nagata, K. (2000). Benzylidene lactam compound, KNK437, a novel inhibitor of acquisition of thermotolerance and heat shock protein induction in human colon carcinoma cells. *Cancer Res.* **60**, 2942-2948.